

Efficient IAM Greybox Penetration Testing

YANG HU*, The University of Texas at Austin, USA

WENXI WANG*, The University of Virginia, USA

SARFRAZ KHURSHID, The University of Texas at Austin, USA

MOHIT TIWARI, The University of Texas at Austin, USA

Identity and Access Management (IAM) is an access control service in cloud platforms. To securely manage cloud resources, customers need to configure IAM to specify the access control rules for their cloud organizations. However, misconfigured IAM can lead to privilege escalation (PE) attacks, causing significant economic loss. Third-party cloud security services detect such issues using whitebox penetration testing, which requires full access to IAM configurations. However, since these configurations often contain sensitive data, customers must manually anonymize them to protect their privacy. To address the dual challenges of anonymization and data privacy, we introduce TAC, the *first* greybox penetration testing approach for third-party services to efficiently detect IAM PEs. Instead of requiring customers to blindly anonymize their entire IAM configuration, TAC intelligently interacts with customers by querying only a small fraction of information in the IAM configuration that is necessary for PE detection. To achieve this, TAC integrates two key innovations: (1) a comprehensive IAM modeling approach to detect a wide range of IAM PEs using partial information collected from query responses, and (2) a query optimization mechanism leveraging Reinforcement Learning (RL) and Graph Neural Networks (GNNs) to minimize customer inputs. Additionally, to address the scarcity of real-world IAM PE datasets, we introduce IAMVulGen, a synthesizer that generates a large number of diverse IAM PEs that mimic real-world scenarios. Experimental results on both synthetic and real-world benchmarks show that TAC, as a greybox approach, achieves competitively low and, in some cases, significantly lower false negative rates than state-of-the-art whitebox approaches, while utilizing a limited number of queries.

1 Introduction

IAM [4] refers to an access control service in cloud platforms. It aims to securely manage the access to resources based on an IAM configuration specified by cloud customers with the access control rules in their cloud organizations. An IAM configuration consists of two components: entities (e.g., users and services such as Amazon EC2 instances) and permissions. Given a service request and an IAM configuration, IAM is able to check if the request obeys or violates the IAM configuration, and decide if the request should be allowed or denied.

Therefore, the correctness of IAM configurations plays an essential role in the effectiveness of cloud access control. Incorrect IAM configurations, namely *IAM misconfigurations*, can cause adverse security consequences such as data breaches, denial of services and resource hijacking [15, 34, 35, 38, 39], which have led to significant economic loss in recent years [33]. IAM Privilege Escalation (PE) [18, 26, 28] is an attack towards cloud access control that exploits the flaws within IAM to obtain additional permissions for performing sensitive operations or accessing sensitive data/resources. One of the most common ways to realize IAM PEs is to exploit IAM misconfigurations: the misconfigured IAM may allow the attacker to modify its configuration so that the attacker is allowed by the modified IAM configuration to obtain additional sensitive permissions.

Cloud security services can be generally classified into two types: *native services* provided by cloud providers [7–11] and *third-party services* offered by startups, labs, and open-source projects [22, 24, 25]. Native services generally offer basic security guarantees, while third-party

*these authors contributed equally to this work.

services cater to customers with more complex and specialized demands [23, 43]. As a result, native services often lack advanced IAM PE detection capabilities, whereas third-party services excel in addressing this critical need.

In this paper, we focus on third-party cloud security services for detecting PEs due to IAM misconfigurations. To our knowledge, all existing third-party services apply *whitebox* penetration testing techniques [19, 21, 30, 31, 42, 44], which require the access to complete IAM configurations. However, sharing the entire IAM configurations to third-party cloud security services can raise a potential security risk in leaking sensitive information of their cloud organizations (e.g., the internal organization architecture). This level of transparency might not be acceptable for cloud customers in fields with elevated security requirements, such as healthcare, finance, and government [29, 36, 41]. To mitigate the security concerns, cloud customers have to anonymize the sensitive information in their IAM configurations before using third-party services, which could take a significant amount of manual efforts.

To avoid both laborious anonymizations and sensitive information disclosure, we propose a first greybox penetration testing approach called TAC to efficiently detect IAM PEs. The idea is to intelligently interact with cloud customers through a sequence of queries, requesting only the essential information needed for the detection. Specifically, each query seeks information about one permission assignment (i.e., whether a particular permission is assigned to a specific entity). During each interaction, customers will be presented with one query and given the option to either accept or decline the query based on their knowledge of whether the query might expose confidential information. In addition, customers are allowed to set up a query budget, which is the maximum number of queries they are willing to interact with. The primary goal of TAC is to detect the IAM PE within the query budget. In particular, to ensure TAC’s practical applicability, TAC needs to minimize customer input, thereby reducing customer’s manual effort and effectively handling PE detection tasks with a limited query budget.

To achieve this goal, TAC needs to tackle two challenging problems: 1) detecting PEs based on partial information of IAM configurations collected by queries, and 2) learning to generate as few queries as possible to perform the detection within the query budget. To solve the first problem, we first propose a comprehensive concrete IAM modeling based on our *Permission Flow Graph*, for detecting a broader class of PEs than the existing whitebox detectors. Furthermore, to detect PE only with partial information during the greybox testing, we propose abstract IAM modeling with predefined abstract states and rules for updating the configuration with partial information provided by the queries. For the second problem of query optimization, we utilize Reinforcement Learning (RL) to pretrain a Graph Neural Network (GNN) based query model, aiming to minimize the number of queries for IAM PE detection.

Pretraining and evaluating TAC require a large number of diverse tasks. To our knowledge, there is only one publicly available IAM PE task set called IAM Vulnerable [1] containing only 31 tasks. Regarding this, we propose an IAM PE task synthesizer called IAMVulGen which generates a large number of IAM PE tasks that mimic real-world scenarios, by leveraging 72 common entity types and 219 permission flow templates manually identified from Amazon Web Services (AWS) official documentation [4–6] and studies on IAM PEs [18, 26, 28, 48].

To evaluate TAC, we used 500 tasks generated by IAMVulGen (unseen in the pretraining), the 31 tasks from the only publicly available IAM PE task set IAM Vulnerable, and two real-world IAM PE tasks collected from a security startup as our evaluation benchmarks. For baselines, since there is no existing greybox or blackbox penetration testing tool for IAM PEs, we take three state-of-the-art whitebox penetration testing tools, namely Pacu [30], Cloudsplaining [42] and PMapper [19] as our baselines. In addition, to understand how our IAM modeling contributes to TAC, we build a whitebox variant of TAC that solely applies our IAM modeling to detect PEs. To assess how our

proposed GNN-based RL with pretraining enhances TAC, we build four greybox variants of TAC, each of which employs a different pretraining strategy or query model.

As a result, on the synthesized IAM PE task set by IAMVulGen, TAC’s whitebox variant successfully detected all PEs, and significantly outperforms all three state-of-the-art whitebox baselines, showing the outstanding effectiveness of our IAM modeling. In addition, given a query budget of 100, TAC identifies 32% to 68% more PEs with 13% to 23% fewer queries on average than all its four greybox variants, demonstrating the superiority of our pretraining based deep RL approach. On the only publicly available task set IAM Vulnerable [1], TAC is able to detect 23 PEs (under a query budget of 10), and all 31 PEs (with a query budget of 20), which substantially outperforms all three whitebox baselines. Furthermore, TAC successfully detects two real-world PEs (with a query budget of 60). The contributions of this paper are:

- **Modeling.** A comprehensive IAM modeling is introduced, providing the foundation of our IAM greybox penetration testing approach.
- **Approach.** To our knowledge, TAC is the first interactive greybox penetration testing tool to detect PEs due to IAM misconfigurations.
- **Synthetic Data.** An IAM PE synthesizer, IAMVulGen, is proposed.

2 Background - IAM Basics

IAM Configurations. IAM configurations consist of entities and permissions. Entities represent subjects (e.g., users, user groups, services) or roles. Subjects actively perform actions, while roles encapsulate job functions and responsibilities within an organization. Permissions define privileges to perform operations and can be assigned directly or indirectly. Direct assignments apply to users, user groups, and roles, while indirect assignments depend on relationships between entities. For instance, a user inherits all permissions assigned to their user group, and a user assuming a role gains all of the role’s permissions.

Figure 1 illustrates an IAM configuration as a relational graph with six entities across four types: one user group (Group 1), two users (User 1, User 2), one service (Service 1), and two roles (Role 1, Role 2); and three permissions: Perm 1, Perm 2, and Perm 3. Entity-permission connections (highlighted in orange) indicate direct assignments: Perm 1 and Perm 2 are assigned to Role 1, Perm 2 to Group 1, and Perm 3 to Role 2. Entity-entity connections (highlighted in blue) represent relationships between entities: user-group (e.g., users in a group), user-role (e.g., a user assuming a role), and service-role (e.g., a service assuming a role). Through these relationships, permissions can be inherited indirectly. For example, User 1 and User 2 in Group 1 indirectly obtain Perm 2, while User 2 and Service 1 indirectly gain Perm 3 by assuming Role 2.

PEs due to Misconfigurations. PE in IAM [18, 26, 28] refers to exploiting IAM flaws to gain unauthorized permissions for sensitive operations or access to sensitive data/resources. A primary cause of PE is IAM *misconfigurations*, which this paper focuses on. Misconfigured IAM can enable attackers to alter configurations, allowing them to obtain additional sensitive permissions. We define the *untrusted entity* as an attacker controlled entity and the *target permission* as the permission the attacker seeks to obtain illegally. PE occurs when the attacker controls the untrusted entity to exploit IAM misconfigurations, assigning the target permission to the untrusted entity.

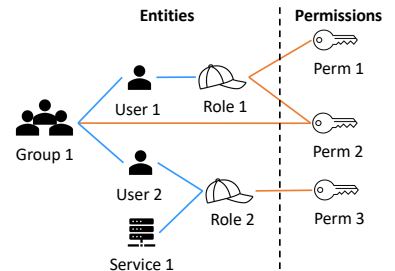


Fig. 1. IAM config. example.

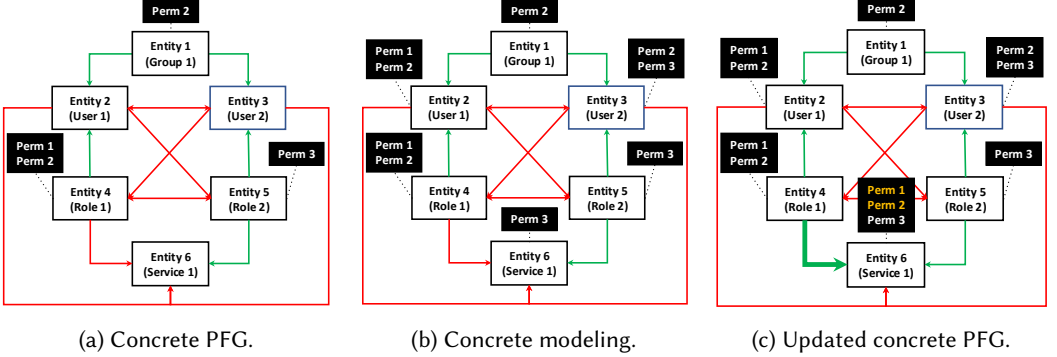


Fig. 3. PFGs of the example in Figure 1; use green for enabled permission flows, red for disabled ones.

Figure 1 presents a crafted misconfiguration, a simplified version of a notorious 2019 IAM PE incident [27, 35], which compromised 100 million Capital One credit card applications and accounts. In the incident, the attacker controls an EC2 instance (Service 1, the untrusted entity) to assume Role 2, which has access to the AWS Metadata Service. The attacker exploits a Server-Side Request Forgery vulnerability of the Metadata Service to obtain a temporary credential (Perm 3) to assume Role 1. From Role 1, the attacker obtains the permission (Perm 1, the target permission) to access an S3 bucket containing sensitive data. In our crafted example, Service 1 indirectly obtains Perm 3 by assuming Role 2 and uses it to assume Role 1, indirectly acquiring the target permission Perm 1.

The example illustrates a *single-step PE*, where the untrusted entity uses one permission to realize PE. However, a more complicated *multi-step PE* (or *transitive PE*) [21, 44] can occur, involving multiple permissions. This paper focuses on detecting both PE types.

3 IAM Modeling

We present our *concrete* IAM modeling using our proposed *Permission Flow Graph*. We further propose our *abstract* IAM modeling, which provides the foundation of our greybox penetration testing approach.

3.1 Concrete IAM Modeling

Permission Flow. We first propose the *permission flow* to model an indirect permission assignment from one entity to another. Each permission flow has a *flow state* representing whether the flow is currently enabled or disabled. If a flow from entity e_1 to entity e_2 is enabled, all permissions assigned to e_1 are automatically assigned to e_2 ; if disabled, they are not.

A permission flow between two entities exists if a relation between the two entity types supports indirect permission assignments. For instance, the user-role relation states that permissions assigned to a role are indirectly assigned to any users assuming that role. In the example from Figure 1, there are four permission flows from Role 1 and Role 2 to User 1 and User 2. Note that the permission flows can be manually extracted based on the semantics of entity-entity relations from

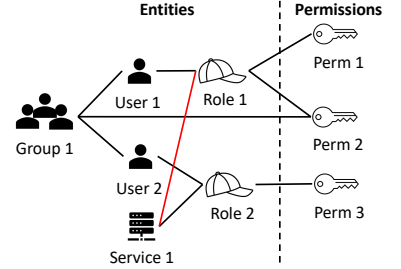


Fig. 2. Modified config. in PE

AWS documentation and relevant studies[5, 18, 26, 28, 48]. Details about identifying permission flows is introduced in Section 6.

The flow state depends on the current relationship between entities. If currently related, the flow is enabled; if not, it is disabled. In the illustrative example (Figure 1), User 1 is related to Role 1 but not Role 2. Figure 3a shows its corresponding flow states: the flow from Role 1 to User 1 is enabled, while the flow from Role 2 to User 1 is disabled.

Permission Space. We identify two types of permissions which the untrusted entity can exploit to obtain the target permission: Type-I and Type-II permissions. A Type-I permission enables a permission flow from entity e_1 to entity e_2 , automatically assigning all permissions of e_1 to e_2 . A Type-II permission directly assigns a Type-I or target permission (denoted as p) to an entity e . For example, adding a user to a user group is a Type-I permission, as it establishes a permission flow; attaching an IAM policy to a user is a Type-II permission, as it directly assigns permissions in the policy to the user.

The permission space in our modeling includes all Type-I permissions (P_I), all Type-II permissions (P_{II}), and the target permission (if neither Type-I nor Type-II). In the example (Figure 1), Perm 1 represents the target permission, Perm 2 is a Type-II permission that allows its assigned entity to directly assign Perm 1 to Role 1, and Perm 3 is a Type-I permission that allows its assigned entity to assume Role 1, enabling a flow from the assigned entity to Role 1.

Permission Flow Graph. We propose the Permission Flow Graph (PFG) to concretely model an IAM configuration, with entities as nodes and permission flows as edges. Formally, a PFG is defined as $G = (E, F, \mathcal{A}, \mathcal{W})$, where E represents the set of entities; $F \subseteq E \times E$ represents permission flows; $\mathcal{A} : E \rightarrow 2^P$ denotes a permission assignment function which maps entities to permissions in the permission space P ; and $\mathcal{W} : F \rightarrow \{\text{true}, \text{false}\}$ indicates whether a flow is enabled (true) or disabled (false). Figure 3a illustrates a PFG which straightforwardly models the IAM configuration in Figure 1. Three entities (Group 1, Role 1, and Role 2) have directly assigned permissions. Based on the semantics of user-role, service-role, and user-group relations, each associated with indirect permission assignments, 12 permission flows are identified. As shown in Figure 1, five of the entity-entity pairs are currently related, thus resulting in five enabled flows, while the remaining seven are disabled.

Concrete Modeling of IAM Configurations. Given a PFG $G = (E, F, \mathcal{A}, \mathcal{W})$, we define a permission flow function \mathcal{M} that generates a new PFG $G' = (E, F, \mathcal{A}', \mathcal{W})$ after one permission flow iteration. Formally, $G' = \mathcal{M}(G)$, where:

$$\mathcal{A}'(e_2) = \bigcup_{\{(e_1, e_2) \in F \mid \mathcal{W}(e_1, e_2) = \text{true}\}} \mathcal{A}(e_1) \cup \mathcal{A}(e_2),$$

meaning that for each entity e_2 , all permissions of entities with enabled flows to e_2 are assigned to e_2 .

To model the IAM configuration, we apply the permission flow function iteratively on G until a fixed point is reached. The resulting PFG, denoted G' , represents the concrete model of the IAM configuration. Formally, $G' = \mathcal{M}^*(G)$, where $\mathcal{M}^*(G) = \mathcal{M}^n(G)$ such that $\mathcal{M}^n(G) = \mathcal{M}^{n-1}(G)$. Figure 3b illustrates the concrete PFG derived from the IAM configuration in Figure 1, representing the fixed point of the PFG in Figure 3a. Based on five enabled permission flows, indirect assignments update the PFG: 1) User 1 and User 2 indirectly obtain Perm 2 from Group 1; 2) User 2 and Service 1 indirectly obtain Perm 3 from Role 2; and 3) User 1 indirectly obtains Perm 1 and Perm 2 from Role 1. The resulting PFG cannot be updated further, as it has reached a fixed point.

Concrete Modeling of IAM PEs. An IAM configuration has a PE iff the untrusted entity can obtain the target permission through its assigned permissions. Formally, let $G_0 = (E_0, F_0, \mathcal{A}_0, \mathcal{W}_0)$

represent the initial IAM configuration, u the untrusted entity, and $l \in P \setminus \mathcal{A}_0(u)$ the target permission. The configuration G_0 has a PE iff there exists a sequence of permissions p_1, \dots, p_n , where $p_i \in \mathcal{A}_{i-1}(u)$, and a modified configuration $G_n = (E_n, F_n, \mathcal{A}_n, \mathcal{W}_n)$ such that

$$G_0 \xrightarrow{p_1} G_1 \dots \xrightarrow{p_n} G_n \wedge l \in \mathcal{A}_n(u),$$

where $G_{i-1} \xrightarrow{p_i} G_i$ indicates that the configuration G_{i-1} is modified to G_i by the untrusted entity u using the permissions $p_i \in \mathcal{A}_{i-1}(u)$.

For example, consider the modeled concrete configuration in Figure 3b, where Service 1 is the untrusted entity and Perm 1 the target permission. When Service 1 applies Perm 3, the permission flow from Role 1 to Service 1 is enabled, assigning all permissions of Role 1 (i.e., Perm 1 and Perm 2) to Service 1. This modification is denoted as $G_0 \xrightarrow{\text{Perm 3}} G_1$, where G_0 is the original configuration, and G_1 , shown in Figure 3c, is the resulting configuration. Since Perm 1 is now assigned to Service 1 ($\text{Perm 1} \in \mathcal{A}_1(\text{Service 1})$), the original configuration G_0 is determined to have a PE.

3.2 Abstract IAM Modeling

The concrete IAM modeling above requires full access to the IAM configuration, but not all permission assignments are necessary for detecting PEs. For example, the PE in Figure 2 can be detected using only partial information: Service 1 owns Perm 3, and Role 1 owns Perm 1. Building on this insight, we propose abstract IAM modeling that identifies PEs using partial permission assignments, forming the basis of our greybox penetration testing technique.

Abstract PFG. The abstract PFG models IAM configurations with partially *visible entities* and *visible permission flows* among them, where flow states are unknown. In the illustrative example, the visible entities are User 1, Role 1, and Service 1, and the visible permission flows are shown in Figure 4.

Using the visible entity space $E_{\text{vis}} \subseteq E$ and the visible permission flow space $F_{\text{vis}} \subseteq F$, we construct a visible permission space $P_{\text{vis}} \subseteq P$. This space includes Type-I and Type-II permissions related to E_{vis} or F_{vis} (i.e., permissions that directly assign permissions to a visible entity or enable a visible permission flow) and the target permission. The abstract PFG is defined as a tuple $\hat{G} = (\hat{E}, \hat{F}, \hat{\mathcal{A}}, \hat{\mathcal{W}})$, where \hat{E} denotes the abstract entity space, \hat{F} denotes the abstract permission flow space, $\hat{\mathcal{A}}$ denotes the abstract entity-permission state function, and $\hat{\mathcal{W}}$ denotes the abstract permission flow state function. Each component is detailed below.

To construct our abstract entity space and permission flow space, we begin by transforming each Type-II permission into a Type-I permission. This transformation simplifies state transitions, as explained later in this section. Recall that a Type-II permission s , when assigned to an entity, allows it to directly assign a target permission or a Type-I permission t_s to an entity e_s . For each Type-II permission s , we 1) add a *pseudo entity* β_s assigned the corresponding target or Type-I permission t_s , and 2) add a *pseudo permission flow* from β_s to the entity e_s . This way, each Type-II permission s becomes a Type-I permission which allows the assigned entity to enable the pseudo permission flow from β_s to e_s . Using these transformations, we define the abstract entity space \hat{E} and abstract flow space \hat{F} by extending the visible entity space E_{vis} and visible flow space F_{vis} with

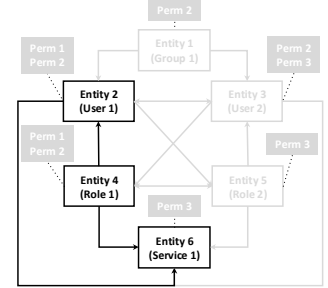


Fig. 4. The visible PFG.

pseudo entities and pseudo flows, respectively. Formally, $\hat{E} = E_{\text{vis}} \cup \{\beta_s | s \in P_{\text{II}} \cap P_{\text{vis}} \wedge e_s \in E_{\text{vis}}\}$, and $\hat{F} = F_{\text{vis}} \cup \{(\beta_s, e_s) | s \in P_{\text{II}} \cap P_{\text{vis}} \wedge e_s \in E_{\text{vis}}\}$.

Next, we define the abstract entity-permission state function $\hat{\mathcal{A}} : \hat{E} \times P_{\text{vis}} \rightarrow \{?, +\}$, which assigns an abstract state to each entity-permission pair. Specifically, $\hat{\mathcal{A}}(e, p) = ?$ means that it is unknown whether permission p can be assigned to entity e . $\hat{\mathcal{A}}(e, p) = +$ means that permission p can be assigned to entity e , either directly or indirectly. Initially, $\hat{\mathcal{A}}$ assigns $?$ to all pairs, except for pseudo entities and their corresponding Type-I or target permissions (involved in the Type-II permission). Formally, the initial state is defined as:

$$\hat{\mathcal{A}}_{\text{init}}(e, p) = \begin{cases} +, & \exists s \in P_{\text{II}} \cap P_{\text{vis}}. e = \beta_s \wedge p = t_s, \\ ?, & \text{otherwise.} \end{cases}$$

The abstract permission flow state function $\hat{\mathcal{W}} : \hat{F} \rightarrow \{*, \oplus\}$ assigns abstract states to permission flows. $\hat{\mathcal{W}}(f) = *$ means that it is unknown whether the permission flow f can be enabled. $\hat{\mathcal{W}}(f) = \oplus$ means that the permission flow f can be enabled. Initially, all permission flows are mapped to $*$, formally defined as $\forall f \in \hat{F}, \hat{\mathcal{W}}_{\text{init}}(f) = *$.

Figure 6a shows an initial abstract PFG $\hat{G}_{\text{init}} = (\hat{E}, \hat{F}, \hat{\mathcal{A}}_{\text{init}}, \hat{\mathcal{W}}_{\text{init}})$, representing the abstract modeling of the visible concrete PFG shown in Figure 4. Recall that Perm 2 is a Type-II permission allowing its assigned entity to directly assign the target permission Perm 1 to Role 1. This is transformed into a Type-I permission by adding a pseudo entity Entity $\beta_{\text{perm 2}}$ and a pseudo flow from Entity $\beta_{\text{perm 2}}$ to Role 1. The abstract entity space is expanded with Entity $\beta_{\text{perm 2}}$, and the abstract permission flow space includes the new pseudo flows. Entity-permission states are initialized to $?$, except for the pseudo entity Entity $\beta_{\text{perm 2}}$ and the target permission Perm 1 (involved in the Type-II permission Perm 2), which are set to $+$. All flow states are initialized to $*$.

Abstract Permission Flow Function. Given an abstract PFG $\hat{G} = (\hat{E}, \hat{F}, \hat{\mathcal{A}}, \hat{\mathcal{W}})$, the abstract permission flow function $\hat{\mathcal{M}}$ performs one permission flow iteration, producing a new PFG $\hat{G}' = (\hat{E}, \hat{F}, \hat{\mathcal{A}}', \hat{\mathcal{W}}')$. Formally, $\hat{G}' = \hat{\mathcal{M}}(\hat{G})$, where:

$$\hat{\mathcal{A}}'(e, p) = \begin{cases} +, & \mathbf{C1:} \exists e' \in N_{\oplus}^{(e)}. \hat{\mathcal{A}}(e', p) = +, \\ \hat{\mathcal{A}}(e), & \text{otherwise.} \end{cases}$$

$$\hat{\mathcal{W}}'(f) = \begin{cases} \oplus, & \mathbf{C2:} \exists p \in P_{\text{I}} \cap P_{\text{vis}}. \llbracket p \rrbracket = f \wedge \hat{\mathcal{A}}(u, p) = +, \\ \hat{\mathcal{W}}(f), & \text{otherwise.} \end{cases}$$

Here, $N_{\oplus}^{(e)} = \{e' | (e', e) \in \hat{F} \wedge \hat{\mathcal{W}}(e', e) = \oplus\}$; $\llbracket p \rrbracket$ refers to the permission flow that can be enabled with the Type-I permission p .

Condition C1 updates the abstract state of an entity-permission pair (shown in Figure 5a). If there exists an entity e' having the permission p (abstract state $+$) and an enabled permission flow (abstract flow state \oplus) from the entity e' to an entity e , then e can have the permission p , updating the state of (e, p) to $+$.

Condition C2 updates the abstract state of a permission flow (shown in Figure 5b). If an untrusted entity u has a permission p (abstract state of (u, p) is $+$), which is a Type-I permission that allows to enable a flow f , then the abstract state of f is updated to \oplus .

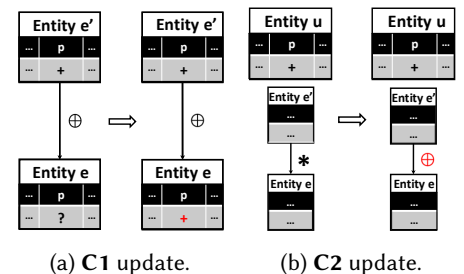


Fig. 5. Abstract state updates

Abstract IAM Configuration Modeling. Similar to concrete IAM configuration modeling, we perform a fixed-point iteration on an abstract PFG \hat{G} using the abstract permission flow function $\hat{\mathcal{M}}$. The resulting PFG \hat{G}' serves as our abstract model of the IAM configuration. Formally, $\hat{G}' = \hat{\mathcal{M}}^*(\hat{G})$, where $\hat{\mathcal{M}}^*$ represents the fixed-point iteration of $\hat{\mathcal{M}}$ (i.e., $\hat{\mathcal{M}}^*(G) = \hat{\mathcal{M}}^n(G)$ such that $\hat{\mathcal{M}}^n(G) = \hat{\mathcal{M}}^{n-1}(G)$).

In particular, the initial abstract PFG $\hat{G}_{\text{init}} = (\hat{E}, \hat{F}, \hat{\mathcal{A}}_{\text{init}}, \hat{\mathcal{W}}_{\text{init}})$, represents the initial abstract IAM configuration. The *terminal* abstract IAM configuration is denoted as $\hat{G}_{\text{term}} = (\hat{E}, \hat{F}, \hat{\mathcal{A}}_{\text{term}}, \hat{\mathcal{W}}_{\text{term}})$, where $\hat{\mathcal{A}}_{\text{term}}(u, l) = +$. All other configurations are considered *intermediate* abstract IAM configurations. Figure 6 illustrates these three types of configurations derived from the partially visible PFG in Figure 4.

4 Greybox Penetration Testing for Detecting IAM PEs

Based on abstract IAM modeling, we propose a greybox penetration testing approach for detecting IAM PEs, without requiring a complete IAM configuration. Unlike existing whitebox penetration testing approaches which force their customers to pay lots of manual efforts to blindly eliminate all sensitive information of their IAM configurations, our greybox approach actively interacts with cloud customers to query only the essential information related to PE detection.

Our approach only requires cloud customers to provide two simple initial inputs beforehand: 1) the type of the untrusted entity and the target permission; and 2) visible entities that customers are inclined to be queried with. We automatically anonymize each visible entity (including the untrusted entity) with randomly generated IDs, construct visible permissions linked to these renamed entities, and define visible permission flows (with unknown states) based on entity types. These elements form the initial abstract IAM configuration. For the illustrative example, suppose the customer chooses User 1, Role 1 and Service 1 as visible entities, they are renamed as Entity 2, Entity 4, and Entity 6, respectively. The initial abstract IAM configuration is shown in Figure 6a.

Our interactive greybox approach delivers one query to the cloud customer at a time, inquiring whether a visible permission is assigned to a visible entity. The cloud customer can choose to either respond to or decline the query, based on their knowledge of whether the inquired permission assignment information is confidential. Formally, let $Q = E_{\text{vis}} \times P_{\text{vis}}$ be the query space. The customer's response for a concrete IAM configuration $G = (E, F, \mathcal{A}, \mathcal{W})$ is defined as a function $O : Q \mapsto \{\text{true, false, unknown}\}$ satisfying

$$O(e, p) = \begin{cases} \text{true,} & \text{accept} \wedge p \in \mathcal{A}(e), \\ \text{false,} & \text{accept} \wedge p \notin \mathcal{A}(e), \\ \text{unknown,} & \neg \text{accept} \end{cases}$$

where *accept* denotes whether the customer accepts to answer the query.

Our approach enables cloud customers to specify the number of queries they are willing to accept, namely the *query budget*. Within this budget, the approach determines whether a PE is detected. An IAM configuration is considered to have a PE iff its initial abstract configuration can be updated to a terminal abstract configuration, based on customer query responses. Formally, let $\hat{G}_0 = (\hat{E}_0, \hat{F}_0, \hat{\mathcal{A}}_0, \hat{\mathcal{W}}_0)$ be the initial abstract IAM configuration, u the untrusted entity, and l the target permission. The initial abstract IAM configuration \hat{G}_0 has a PE iff there exists a sequence of queries $(e_1, p_1), \dots, (e_n, p_n) \in Q$, and a terminal abstract IAM configuration $\hat{G}_n = (\hat{E}_n, \hat{F}_n, \hat{\mathcal{A}}_n, \hat{\mathcal{W}}_n)$ such that

$$\hat{G}_0 \xrightarrow{(e_1, p_1)} \hat{G}_1 \dots \xrightarrow{(e_n, p_n)} \hat{G}_n \wedge \hat{\mathcal{A}}_n(u, l) = +,$$

where $\hat{G}_{i-1} \xrightarrow{(e_i, p_i)} \hat{G}_i$ annotates that the abstract IAM configuration \hat{G}_{i-1} is updated to \hat{G}_i based on the customer response to the query (e_i, p_i) :

$$\hat{G}_i = \begin{cases} \hat{M}^*(\hat{G}_{i-1}[\hat{\mathcal{A}}_{i-1}[e_i, p_i] \mapsto +]), & O(e_i, p_i) = \text{true}, \\ \hat{G}_{i-1}, & \text{otherwise.} \end{cases}$$

Our abstract IAM modeling and state updating rules ensure the precision of IAM PE detection, meaning that any PEs which are identified by TAC are guaranteed to be valid.

We use the illustrative example in Figure 6 to demonstrate how TAC interacts with a customer through queries to detect IAM PEs. Starting with the initial abstract IAM configuration in Figure 6a, our approach may query whether Entity 6 initially has Perm 3 (query: (Entity 6, Perm 3)). The customer responds true (i.e., $O(\text{Entity 6, Perm 3}) = \text{true}$), updating the abstract state of (Entity 6, Perm 3) to +. Since Perm 3 is the Type-I permission which allows its assigned entity (i.e., Entity 6) to enable the flow from Entity 4 to Entity 6. Thus, the abstract state of this flow is updated to \oplus , resulting in the intermediate abstract IAM configuration shown in Figure 6b. Next, our approach may query whether Entity 4 has the target permission Perm 1 (query: (Entity 4, Perm 1)). The customer again responds true (i.e., $O(\text{Entity 4, Perm 1}) = \text{true}$), updating the state of (Entity 4, Perm 1) to +. According to condition C1 of the abstract permission flow function \hat{M} , the state of (Entity 6, Perm 1) is also updated to +. Since the initial IAM configuration can be updated to the terminal abstract IAM configuration in Figure 6c, the configuration is confirmed to have a PE.

5 Efficient IAM Greybox Penetration Testing

To make our greybox testing approach practical, we focus on improving efficiency by minimizing the customer's manual inputs, specifically reducing the number of query responses. This requires detecting IAM PEs with as few queries as possible within the specified query budget. The problem is a *sequential decision-making* problem, where each query is selected based on the customer's responses to previous queries. For instance, in the example in Figure 6, if the response to the first query confirms that Entity 6 has Perm 3, it makes sense to follow up with a second query about whether Entity 4 has Perm 1. This is because Perm 3 could enable a permission flow from Entity 4 to Entity 6, potentially assigning Perm 1 to Entity 6, thereby revealing a PE. However, if the response shows that Entity 6 does not have Perm 3, the

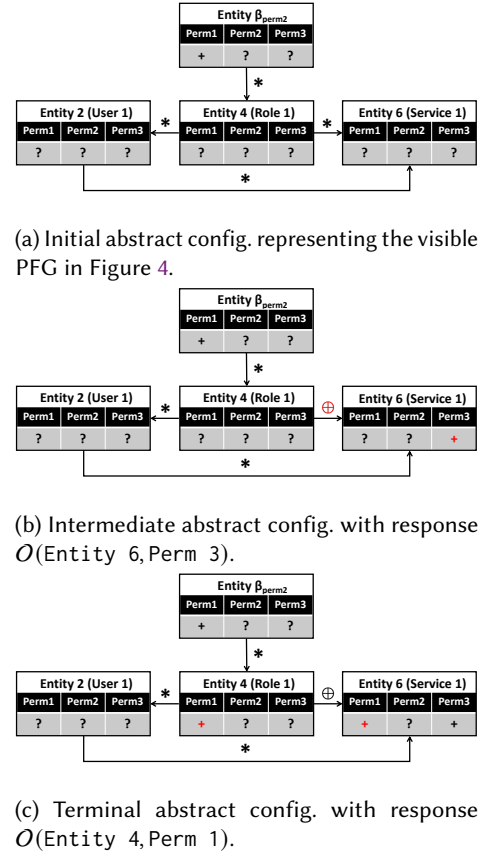


Fig. 6. An example for IAM interactive greybox penetration testing.

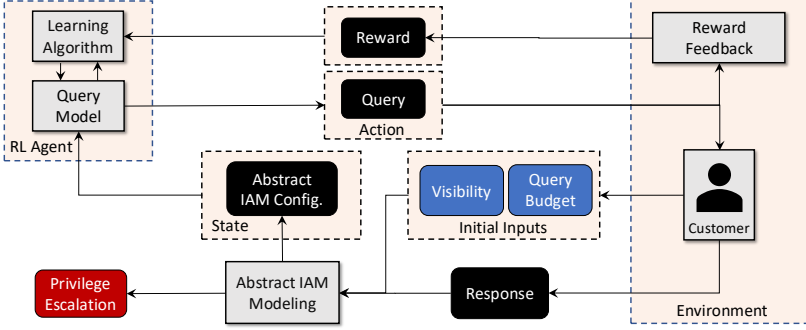


Fig. 7. The general framework of TAC.

second query would be inefficient for revealing any PEs. In that case, a different query should be selected for PE detection.

To address the sequential decision-making problem, we propose an efficient greybox approach called TAC, which leverages RL to minimize the number of queries required to detect IAM PEs.

5.1 Overview

The framework of TAC is based on our RL formulation of the problem, as illustrated in Figure 7. In each episode, the RL agent starts with its visibility, an initial abstract IAM configuration, and a query budget. The agent iteratively sends queries to update the abstract IAM configuration until either a PE is identified or the query budget is reached. At each step, the agent uses a *query model* (i.e., the RL policy) to select a query (i.e., the action) based on the current abstract IAM configuration (i.e., the state). In the RL environment, the abstract IAM configuration is updated based on the customer's query response, and a reward of -1 per query is provided by a reward feedback module. The RL agent uses the classic Actor-Critic Method [47] to update the query model based on the feedback. The objective of the RL agent is to learn an optimal query model that maximizes the return (i.e., cumulative rewards), effectively minimizing the number of queries needed.

Our RL formulation requires the agent to detect a PE within a single episode. However, classic deep RL approaches [47], which train policies from scratch with randomly initialized weights, typically require numerous episodes to maximize returns. Inspired by recent advances in zero-shot and few-shot learning for language models [13, 37], we pretrain our query model on a diverse set of PE tasks using *multi-task* RL across multiple episodes. This pretraining aims to improve the model's query efficiency on new PE tasks within a single episode.

However, existing multi-task RL techniques [14, 46] usually suffer from the negative transfer issue, where training on some tasks adversely affects performance on others [40, 45]. To address this, we use domain knowledge in IAM

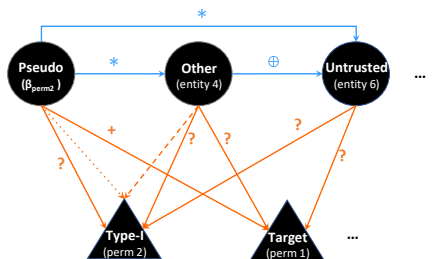


Fig. 8. Graph representation of the abstract config. in Figure 6b. Entity nodes are circles, permission nodes are triangles, entity-entity edges (flows) are blue, and entity-permission edges are orange. Solid lines indicate permission assignments; dotted and dashed lines represent edges from the source or sink of a Type-I flow to the Type-I permission.

PE detection to partition the PE task space into subspaces, grouping tasks that are less likely to interfere with one another. A specialized query model is then pretrained for each subspace. Further details on the query model design and our approach to mitigating negative transfer are discussed as follows.

5.2 Query Model

Our query model generates embeddings for each query based on the current state of the abstract IAM configuration. These embeddings are used to infer a probability distribution over the query space, guiding the selection of the next query. Leveraging the inherently graph-structured nature of IAM configurations (Figure 6), we encode them into graph representations and apply GNNs to generate the query embeddings.

GNNs are particularly well-suited for this task due to their ability to process and generalize across diverse graph structures, enabling pretraining across a wide range of PE tasks from different subspaces. Additionally, GNNs are efficient at handling large-scale graphs, processing millions of nodes and edges using moderate GPU resources. This scalability allows the query model to manage real-world IAM configurations with millions of entities, permissions, and permission flows. Further details on the graph representations, model architecture, and pretraining process are provided in the following subsection.

The Graph Representation. In this subsection, we describe how an abstract IAM configuration is transformed into a directed graph representation, which serves as input for our GNN-based query model. The graph nodes are classified into two main types: entity nodes and permission nodes. Entity nodes are further divided into three subtypes: pseudo entities, untrusted entities, and other entities. Permission nodes are categorized as target permissions or Type-I permissions (all Type-II permissions are converted into Type-I permissions, as explained in Section 3.2). The directed edges in the graph are generally classified into two types, entity-entity type representing permission flows, and entity-permission type including three sub-types: (1) edges representing permission assignments from an entity to one of its assigned permissions; (2) edges from a source entity of a Type-I permission flow to the corresponding Type-I permission; and (3) edges from the sink entity of a Type-I permission flow to the corresponding Type-I permission. Each permission assignment edge in subtype (1) with an unknown abstract state (?) represents a potential query. Node and edge features include their corresponding types. Additionally, edges representing permission flows and assignments carry their abstract values, \hat{W} and \hat{A} , respectively. Figure 8 illustrates the graph representation of the abstract IAM configuration shown in Figure 6b.

GNN-based Model Design. Given the graph representation of the abstract IAM configuration, the GNN-based query model selects an entity-permission edge with an abstract state ? (unknown) based on the inferred probability distribution. It then outputs the corresponding query for the selected edge. The goal of the model is to predict permission assignments with unknown states that are most critical for PE detection.

Figure 9 illustrates the design and workflow of our GNN-based query model. Starting with a graph representation of an abstract IAM configuration (A), five stacked Graph Attention Network (GATv2) layers [12] generate embeddings for permission assignment edges (B). A Multi-Layer Perceptron (MLP) then predicts a probability distribution over query edges (permission assignment edges with an abstract state ?), as shown in (C). Finally, a query edge is selected based on the predicted distribution and converted into a query corresponding to the selected entity and permission. For example, in Figure 9, the edge from Entity 4 to Perm 1 is selected due to its highest probability, resulting in the query (Entity 4, Perm 1) as the output of the model.

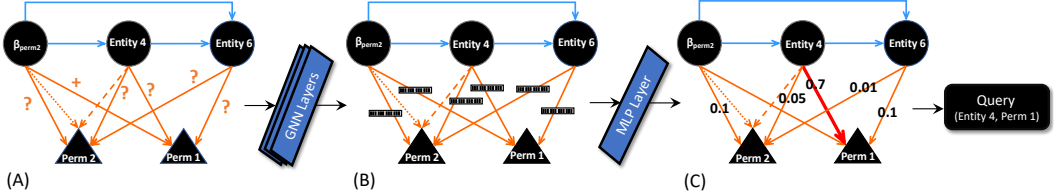


Fig. 9. The design and workflow of the query model.

Model Pretraining. To address the negative transfer issue mentioned in Section 5.1, our intuition is that PE tasks involving the same untrusted entity type are likely to share similar optimal query policies for detecting PEs. Therefore, they are unlikely to interfere with each other during model pretraining. Based on this intuition, we pretrain a query model on PE tasks with the same untrusted entity type. Specifically, given a set of pretraining tasks, we first divide them into groups according to their untrusted entity types. For each group, we pretrain a distinct query model specialized for handling PE tasks with that specific untrusted entity type. This is achieved using RL with a sequential task scheduling strategy, where PE tasks in the group are randomly shuffled and sequentially used to optimize the query model over multiple episodes per task.

6 IAMVulGen - IAM PE Synthesizer

Our pretraining and evaluation processes require a large, diverse, and challenging set of IAM PE tasks. However, the only publicly available dataset, IAM Vulnerable [1], contains just 31 relatively simple tasks. To overcome this limitation, we developed IAMVulGen, a tool designed to generate diverse and realistic IAM PE tasks reflective of real-world scenarios.

To achieve this, we manually identified 72 common entity types and extracted 219 permission flow templates from official AWS documentation [4–6] and studies on IAM PEs [18, 26, 28, 48]. These templates define possible permission flows between different entity types. For example, one template specifies that permissions flow from a user group to its members, as AWS documentation states that permissions assigned to a group are automatically inherited by its users. By leveraging these templates, IAMVulGen ensures the generated data reflects real-world IAM configurations. The identified entity types and templates create thousands of potential entities and millions of possible permissions, enabling IAMVulGen to synthesize IAM misconfigurations of any desired size within this space. IAMVulGen generates each IAM PE task in two steps: (1) creating a concrete IAM misconfiguration and (2) constructing the corresponding initial abstract IAM misconfiguration. The details of these steps are described below.

Step 1: Concrete Misconfiguration Generation. To generate a concrete IAM misconfiguration with PE, IAMVulGen constructs a PFG $G = (E, F, \mathcal{A}, \mathcal{W})$ by generating its components step by step.

1) **Entity space E :** Based on 72 manually identified common entity types, including user, user group, role, and 69 service types, IAMVulGen uniformly samples n entity types ($n \in [1, 5]$ by default) from these categories. For each selected type, it generates m entities ($m \in [1, 20]$ by default).

2) **Permission flow space F :** Using 219 manually extracted permission flow templates, which define entity pairs that can have permission flows, IAMVulGen generates permission flows for all entity pairs in E that matches the templates.

3) **Permission assignment \mathcal{A} :** IAMVulGen first generates the permission space P , which includes Type-I, Type-II, and target permissions. A Type-I permission is created for each permission flow to enable it. For Type-II permissions, three entity types (i.e., user, user group and role) are identified which can be directly assigned with a Type-I/target permission; for each entity with one

of these types and each Type-I/target permission, IAMVulGen generates a Type-II permission for assigning the Type-I/target permission to the entity. Target permissions, such as those granting access to sensitive S3 buckets, are manually identified from AWS IAM security best practices [6] and studies [18, 26, 28, 48]. Using the generated permission space P , IAMVulGen assigns γ_p ($\gamma_p = 20\%$ by default) of the permissions to each entity, uniformly sampled from P .

4) Flow state function W : the state of each permission flow is set to true with a probability of γ_w ($\gamma_w = 0.2$ by default).

Finally, the fixed-point iteration is applied to the generated PFG, producing the final concrete IAM configuration.

Using the generated IAM configuration, IAMVulGen uniformly selects an entity and a permission from the generated entity and permission spaces to serve as the untrusted entity and the target permission, respectively. It then applies three state-of-the-art whitebox PE detectors to check for a PE in the configuration. If at least one detector identifies a PE, the concrete misconfiguration is finalized; otherwise, the process repeats with a new configuration.

Step 2: Initial Abstract Misconfiguration Generation. Based on the created concrete misconfiguration, IAMVulGen creates the corresponding initial abstract IAM misconfiguration by uniformly sampling γ_v ($\gamma_v = 20\%$ by default) of the entities from the concrete misconfiguration as visible entities.

7 Evaluation

7.1 Experimental Setup

PE Task Sets. For pretraining, we generate a task set, `Pretrain`, containing 2,000 IAM PE tasks created by IAMVulGen under its default settings. For evaluation, we use three distinct test sets: (1) `Test-A`, with 500 tasks generated by IAMVulGen; (2) `Test-B`, with 31 tasks from the public IAM PE benchmark `IAM Vulnerable` [1]; (3) `Test-C`, with two large real-world misconfigurations collected from a cloud security startup. None of the testing and pretraining sets have overlap with each other. Appendix A shows details about these sets.

Customer Query Response Simulation. TAC interacts with cloud customers to detect IAM PEs. To evaluate its performance across hundreds of PE tasks, we develop a customer query response simulator. For each IAM PE task, the simulator randomly samples queries from the query space to represent those customers are accept to answer. Given an IAM configuration and a query selected by TAC, the simulator determines whether to accept the query based on the sampled query set and provides an answer using the concrete configuration.

Baselines. Given the lack of publicly available greybox or blackbox IAM PE detectors, we use three state-of-the-art open-source whitebox PE detectors as baselines: `Pacu` [30], `Cloudsplaining` [42], and `PMapper` [19]. To evaluate TAC’s IAM concrete modeling, we include its whitebox variant, `TAC-WB`, which applies only concrete IAM modeling for PE detection. To assess the impact of our GNN-based RL approach, we introduce two greybox variants: `TAC-RD`, which randomly selects queries, and `TAC-EA`, which uses a query model trained with the evolutionary algorithm `CMA-ES` [20]. We also analyze the effect of pretraining on query model performance with `TAC-NoPT`, where the model is not pretrained. Lastly, to study how our pretraining mitigates negative transfer, we include `TAC-MamlPT`, which uses the multi-task RL technique `MAML` [16] for pretraining.

Evaluation Metrics. To evaluate TAC’s effectiveness, we use the false negative rate (FNR) of the IAM PE detection as the metric. False positive rates are not measured since all detectors in our experiments are *precise*, ensuring all detected PEs are true. For efficiency evaluation, we use the *query count*, representing the number of queries used to interact with customers during detection.

Query Budgets. In real-world scenarios, customers determine the query budget based on their willingness to answer queries. A larger budget provides TAC with more information, improving its ability to detect PEs. To challenge TAC and evaluate its performance, we use smaller query budgets here. For Test-A and Test-C task sets, we set 10 query budgets: 10, 20, ..., 100, which are significantly smaller than the maximum query space size of 8,448. For Test-B task set, with a maximum query space size of 27, we use two query budgets: 10 and 20.

Hyper-Parameter Settings. During pretraining, each task is used for 20 episodes to train the query model. The AdamW optimizer [32] with a learning rate of 10^{-4} is applied for both pretraining and testing. To ensure reliable results, all experiments, including pretraining and testing, are repeated 11 times.

7.2 Research Questions

We evaluate effectiveness of our IAM modeling and TAC through the following research questions:

RQ1: How effective is our concrete IAM modeling?

RQ2: How effective is TAC in terms of FNR?

RQ3: How effective is TAC in terms of query count?

Note that the overall effectiveness of TAC, as examined in RQ2 and RQ3, reflects the impact of our abstract IAM modeling.

7.3 Experimental Results

RQ1: Effectiveness of Concrete IAM Modeling. To evaluate our concrete IAM modeling, we tested all three whitebox baselines and TAC-WB on the Test-A, Test-B, and Test-C task sets. TAC-WB detected all PEs across the three sets, achieving a zero FNR. In contrast, on Test-A, the FNRs for PMapper, Pacu, and Cloudsplaining were 12%, 20%, and 26%, respectively. On Test-B, their rates increased to 29%, 32%, and 39%. For Test-C, all three failed to detect either PE, resulting in a 100% FNR. Our manual inspection revealed that FNRs in pattern-based detectors (Pacu and Cloudsplaining) were due to missing relevant PE patterns, while those in the graph-based detector (PMapper) stemmed from limited graph representation expressiveness. *Overall, the zero FNR of TAC-WB highlights the significant advantages of our concrete modeling.*

RQ2: Effectiveness of TAC in FNR. Figure 10a illustrates the FNRs of TAC on the Test-A set, compared to four whitebox baselines and its four greybox variants across 10 query budgets. As the query budget increases from 10 to 100, TAC’s FNR drops significantly from 57% to 27%, consistently outperforming its greybox variants. Additionally, the near-zero standard deviation of TAC’s FNR highlights its superior stability over the greybox variants. These findings demonstrate the effectiveness of both the GNN-based RL approach and pretraining in improving TAC. Compared to whitebox baselines, TAC achieves a FNR of 27% under a query budget of 100, closely matching Cloudsplaining (26%) and only 6% and 14% higher than Pacu and PMapper, respectively. This result underscores TAC’s strong performance as a greybox detector with limited information. Encouraged by these results, we further increased TAC’s query budget, finding that it outperforms all three whitebox baselines when the budget reaches 258. This demonstrates the superiority of our IAM modeling approach, which accounts for a broader class of PEs than the state-of-the-art whitebox baselines. *Overall, the results confirm that TAC achieves competitive effectiveness on the Test-A set, outperforming its greybox variants and rivaling whitebox baselines.*

On the Test-B set, TAC detects 23 PEs with a query budget of 10 (3% FNR) and all 31 PEs with a budget of 20 (0% FNR), outperforming three whitebox baselines (29%-39% FNRs) and matching TAC-WB. In contrast, TAC’s greybox variants detect 17–22 PEs with a budget of 10 (29%-45% FNRs) and 23–30 PEs with a budget of 20 (3%-26% FNRs). On the Test-C set, TAC detects both PEs with

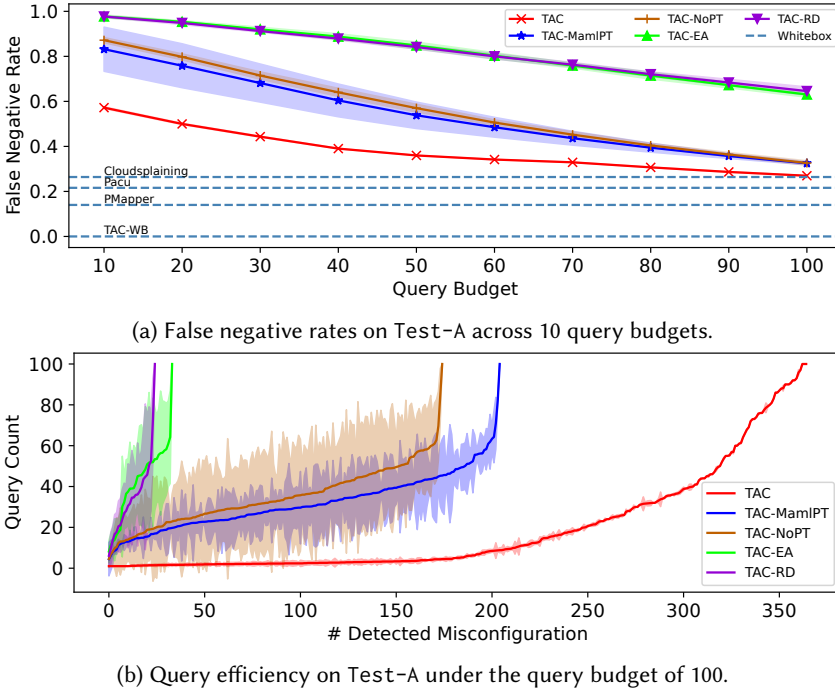


Fig. 10. Evaluation results on Test-A. Solid lines represent the mean, and shaded regions indicate the standard deviation across 11 repeated experiments.

a query budget of 60, while all greybox variants fail at any budget. *In summary*, TAC achieves the lowest FNRs on both Test-B and Test-C sets.

RQ3: Effectiveness of TAC in query count. To evaluate how our GNN-based RL with pretraining improves query efficiency, we compare TAC with its greybox variants in terms of query count. Figure 10b illustrates the query counts of TAC and its greybox variants under a query budget of 100 on the Test-A set. For clarity, detected PEs are sorted for each detector by their average query count, computed from 11 repeated experiments, in ascending order.

We observe that TAC consistently requires significantly fewer queries than its greybox variants to detect the same number of PEs. Conversely, for the same query count, TAC detects far more PEs. Specifically, TAC detects 362 PEs with an average query count of 19, whereas TAC-NoPT detects only 175 PEs with an average query count 1.8 times higher, TAC-MamlPT detects 204 PEs with a count 1.7 times higher, TAC-EA detects only 34 PEs with a count 2.2 times higher, and TAC-RD performs even worse than TAC-EA. Moreover, all four variants show much higher standard deviations than TAC. These results underscore the critical role of our GNN-based RL with pretraining in reducing and stabilizing query counts while mitigating negative transfer. *In summary*, the GNN-based RL with pretraining is essential for enhancing and stabilizing TAC’s query efficiency.

8 Related Work

Existing cloud security tools primarily focus on whitebox IAM PE detection, which can be classified into three categories: reasoning-based approaches, pattern-based approaches, and graph-based approaches.

For reasoning-based approaches, Ilia and Oded [44] employ bounded model checking to formally verify PEs in IAM configurations, by formulating the problem into SMT formulas and uses SMT solver to solve the formula. Unfortunately, as of submission, the reasoning-based detector is not publicly available, preventing its inclusion as a baseline in our experiments. In the pattern-based approach, Gietzen identified 21 typical IAM PE patterns [18]. Tools like Pacu[30] and Cloudsplaining[42] leverage these patterns to detect IAM PEs. However, they cannot identify *transitive PEs*, where attackers gain permissions indirectly through intermediate entities [2].

Graph-based approaches address this limitation. PMapper[19] models authentication relationships between users/roles in IAM configurations as directed graphs, enabling the detection of transitive PEs where non-admin users can authenticate as admins. AWSPEX[31] extends this by visualizing detected PEs. However, these methods have two key drawbacks: (1) they focus solely on user/role authentication, ignoring PEs involving other entity types (e.g., services) or non-authentication strategies (e.g., changing IAM policy versions [3]); and (2) they overlook PEs arising from sensitive permissions in non-admin entities. In contrast, TAC proposes a more general and flexible graph-based approach using our permission flow concepts. This enables detection of diverse PE scenarios beyond authentication chains, including group memberships and role assumption chains, across admin and non-admin entities. Additionally, TAC’s abstract IAM modeling, built on top of its concrete modeling, allows detection with partial visible IAM configuration information.

9 Conclusion

In this paper, we presented TAC, an efficient greybox penetration testing approach for third-party cloud security services to detect IAM PEs caused by misconfigurations. Unlike whitebox methods requiring full anonymization of IAM configurations, TAC selectively queries only essential information. Leveraging a comprehensive IAM modeling framework and a GNN-based RL approach with pretraining, TAC minimizes query usage while detecting a wide range of PEs in partially visible configurations. To create diverse and realistic IAM PE benchmarks, we developed IAMVulGen, an IAM PE task synthesizer. Experimental results on synthetic and real-world benchmarks demonstrate that TAC achieves low, and in some cases even significantly lower, false negative rates compared to state-of-the-art whitebox approaches.

References

- [1] Seth Art. 2021. IAM Vulnerable - An AWS IAM Privilege Escalation Playground. <https://bishopfox.com/blog/aws-iam-privilege-escalation-playground>.
- [2] Seth Art. 2021. IAM Vulnerable - Assessing the AWS Assessment Tools. <https://bishopfox.com/blog/assessing-the-aws-assessment-tools>.
- [3] AWS. 2023. AWS IAM API Reference: SetDefaultPolicyVersion. https://docs.aws.amazon.com/IAM/latest/APIReference/API_SetDefaultPolicyVersion.html.
- [4] AWS. 2023. AWS Identity and Access Management (IAM). <https://aws.amazon.com/iam/>.
- [5] AWS. 2023. AWS Service Authorization Reference: Actions, resources, and condition keys for AWS services. https://docs.aws.amazon.com/pdfs/service-authorization/latest/reference/service-authorization.pdf#reference_policies_actions-resources-contextkeys.
- [6] AWS. 2023. Security best practices in IAM. <https://docs.aws.amazon.com/IAM/latest/UserGuide/best-practices.html>.
- [7] AWS. 2023. Testing IAM policies with the IAM policy simulator. https://docs.aws.amazon.com/IAM/latest/UserGuide/access_policies_testing-policies.html.
- [8] AWS. 2023. Using AWS IAM Access Analyzer. <https://docs.aws.amazon.com/IAM/latest/UserGuide/what-is-access-analyzer.html>.
- [9] AWS. 2023. What is Amazon Verified Permissions? <https://docs.aws.amazon.com/verifiedpermissions/latest/userguide/what-is-avp.html>.
- [10] John Backes, Pauline Bolignano, Byron Cook, Catherine Dodge, Andrew Gacek, Kasper Luckow, Neha Rungta, Oksana Tkachuk, and Carsten Varming. 2018. Semantic-based automated reasoning for AWS access policies using SMT. In *2018 Formal Methods in Computer Aided Design (FMCAD)*. IEEE, 1–9.

- [11] Malik Bouchet, Byron Cook, Bryant Cutler, Anna Druzkina, Andrew Gacek, Liana Hadarean, Ranjit Jhala, Brad Marshall, Dan Peebles, Neha Rungta, et al. 2020. Block public access: trust safety verification of access control policies. In *Proceedings of the 28th ACM Joint Meeting on European Software Engineering Conference and Symposium on the Foundations of Software Engineering*. 281–291.
- [12] Shaked Brody, Uri Alon, and Eran Yahav. 2021. How attentive are graph attention networks? *arXiv preprint arXiv:2105.14491* (2021).
- [13] Tom Brown, Benjamin Mann, Nick Ryder, Melanie Subbiah, Jared D Kaplan, Prafulla Dhariwal, Arvind Neelakantan, Pranav Shyam, Girish Sastry, Amanda Askell, et al. 2020. Language models are few-shot learners. *Advances in neural information processing systems* 33 (2020), 1877–1901.
- [14] Myungsik Cho, Whiyoung Jung, and Youngchul Sung. 2022. Multi-task reinforcement learning with task representation method. In *ICLR 2022 Workshop on Generalizable Policy Learning in Physical World*.
- [15] Cybersecurity Insiders. 2021. Cloud Security Report. <https://www.isc2.org/Landing/cloud-security-report>.
- [16] Tristan Deleu and Yoshua Bengio. 2018. The effects of negative adaptation in model-agnostic meta-learning. *arXiv preprint arXiv:1812.02159* (2018).
- [17] Carlo D’Eramo, Davide Tateo, Andrea Bonarini, Marcello Restelli, and Jan Peters. 2024. Sharing knowledge in multi-task deep reinforcement learning. *arXiv preprint arXiv:2401.09561* (2024).
- [18] Spencer Gietzen. 2018. AWS IAM Privilege Escalation – Methods and Mitigation. <https://rhinosecuritylabs.com/aws/aws-privilege-escalation-methods-mitigation/>.
- [19] NCC Group. 2023. Principal Mapper. <https://github.com/nccgroup/PMapper>.
- [20] Nikolaus Hansen. 2006. The CMA evolution strategy: a comparing review. *Towards a new evolutionary computation* (2006), 75–102.
- [21] Yang Hu, Wenxi Wang, Sarfraz Khurshid, Kenneth L McMillan, and Mohit Tiwari. 2023. Fixing Privilege Escalations in Cloud Access Control with MaxSAT and Graph Neural Networks. 104–115 pages.
- [22] Orca Security Inc. 2024. Thrive Security in the Cloud. <https://orca.security/>.
- [23] Sysdig Inc. 2024. Cloud-Native vs. Third-Party Cloud Security Tools. <https://sysdig.com/learn-cloud-native/cloud-security/cloud-native-vs-third-party-cloud-security-tools/>.
- [24] Symmetry Systems Inc. 2024. Data Security Posture Management. <https://www.symmetry-systems.com/>.
- [25] Wiz Inc. 2024. Secure Everything You Build And Run in the Cloud. <https://go.wiz.io/>.
- [26] Eric Kedrosky. 2022. Achieving AWS Least Privilege: Understanding Privilege Escalation. <https://sonraisecurity.com/blog/common-methods-aws-privilege-escalation/>.
- [27] Shaharyar Khan, Ilya Kabanov, Yunke Hua, and Stuart Madnick. 2022. A systematic analysis of the capital one data breach: Critical lessons learned. *ACM Transactions on Privacy and Security* 26, 1 (2022), 1–29.
- [28] Gerben Kleijn. 2022. Well, That Escalated Quickly: Privilege Escalation in AWS. <https://bishopfox.com/blog/privilege-escalation-in-aws>.
- [29] Manjur Kolhar, Mosleh M Abu-Alhaj, and Saied M Abd El-atty. 2017. Cloud data auditing techniques with a focus on privacy and security. *IEEE Security & Privacy* 15, 1 (2017), 42–51.
- [30] Rhino Security Lab. 2022. Pacu: The Open Source AWS Exploitation Framework. <https://rhinosecuritylabs.com/aws/pacu-open-source-aws-exploitation-framework/>.
- [31] WithSecure Labs. 2022. A graph-based tool for visualizing effective access and resource relationships in AWS environments. <https://github.com/WithSecureLabs/awspx>.
- [32] Ilya Loshchilov and Frank Hutter. 2017. Decoupled weight decay regularization. *arXiv preprint arXiv:1711.05101* (2017).
- [33] Trend Micro. 2021. The Most Common Cloud Misconfigurations That Could Lead to Security Breaches. <https://www.trendmicro.com/vinfo/us/security/news/virtualization-and-cloud/the-most-common-cloud-misconfigurations-that-could-lead-to-security-breaches>.
- [34] Assaf Morag. 2021. Cloud Misconfigurations: The Hidden but Preventable Threat to Cloud Data. <https://www.infosecurity-magazine.com/opinions/cloud-misconfigurations-threat/>.
- [35] Capital One. 2022. Information on the Capital One Cyber Incident. <https://www.capitalone.com/digital/facts2019/>.
- [36] Momen Oqaily, Yoss Jarraya, Meisam Mohammady, Suryadipta Majumdar, Makan Pourzandi, Lingyu Wang, and Mourad Debbabi. 2019. SegGuard: segmentation-based anonymization of network data in clouds for privacy-preserving security auditing. *IEEE Transactions on Dependable and Secure Computing* 18, 5 (2019), 2486–2505.
- [37] Long Ouyang, Jeffrey Wu, Xu Jiang, Diogo Almeida, Carroll Wainwright, Pamela Mishkin, Chong Zhang, Sandhini Agarwal, Katarina Slama, Alex Ray, et al. 2022. Training language models to follow instructions with human feedback. *Advances in Neural Information Processing Systems* 35 (2022), 27730–27744.
- [38] Cedric Pernet. 2021. Research reveals that IAM is too often permissive and misconfigured. <https://www.techrepublic.com/article/research-iam-permissive-misconfigured/>.

- [39] Nathaniel Quist. 2021. Unit 42 Cloud Threat Report Update: Cloud Security Weakens as More Organizations Fail to Secure IAM. <https://unit42.paloaltonetworks.com/iam-misconfigurations/>.
- [40] Michael T Rosenstein, Zvika Marx, Leslie Pack Kaelbling, and Thomas G Dietterich. 2005. To transfer or not to transfer. In *NIPS 2005 workshop on transfer learning*, Vol. 898.
- [41] Jungwoo Ryoo, Syed Rizvi, William Aiken, and John Kissell. 2013. Cloud security auditing: challenges and emerging approaches. *IEEE Security & Privacy* 12, 6 (2013), 68–74.
- [42] Salesforce. 2022. Cloudsplaining. <https://cloudsplaining.readthedocs.io/en/latest/>.
- [43] Hemani Sehgal. 2021. Cloud Security Conundrum Debunked: Native Vs. Third-Party Tools. <https://www.horangi.com/blog/cloud-security-native-third-party-tools>.
- [44] Ilia Shevrin and Oded Margalit. 2023. Detecting {Multi-Step}{IAM} Attacks in {AWS} Environments via Model Checking. In *32nd USENIX Security Symposium (USENIX Security 23)*. 6025–6042.
- [45] Trevor Standley, Amir Zamir, Dawn Chen, Leonidas Guibas, Jitendra Malik, and Silvio Savarese. 2020. Which tasks should be learned together in multi-task learning?. In *International conference on machine learning*. PMLR, 9120–9132.
- [46] Lingfeng Sun, Haichao Zhang, Wei Xu, and Masayoshi Tomizuka. 2022. Paco: Parameter-compositional multi-task reinforcement learning. *Advances in Neural Information Processing Systems* 35 (2022), 21495–21507.
- [47] Richard S Sutton and Andrew G Barto. 2020. *Reinforcement learning: An introduction*. MIT press.
- [48] Xscaler. 2021. Anatomy of a Cloud Breach: How 100 Million Credit Card Numbers Were Exposed. <https://www.zscaler.com/resources/white-papers/capital-one-data-breach.pdf>.

A Task Set Statistics

Task Set	Source	# Task	# Entity Type	# Vis Entity			# Vis Flow			# Permission		
				min	max	avg	min	max	avg	min	max	avg
Pretrain	IAMVulGen	2,000	72	2	34	15	2	274	48	6	313	67
Test-A	IAMVulGen	500	72	3	27	14	2	300	70	12	322	72
Test-B	IAM Vulnerable	31	11	1	3	2	0	6	2	3	12	7
Test-C	Startup	2	8	15	25	20	84	261	172	88	252	170

Table 1. Statistics of three PE task sets.

Table 1 summarizes the statistics of the task sets we have used for pretraining and evaluating TAC. The Pretrain set includes diverse PE tasks with 72 entity types, 2–34 visible entities, 2–274 permission flows, and 6–313 permissions, similar to Test-A. In contrast, Test-B features smaller, less diverse tasks with 11 entity types, 1–3 visible entities, 0–6 permission flows, and 3–12 permissions. The Test-C task set includes two real-world misconfigurations, Real-1 (15 entities, 84 permission flows, 88 permissions) and Real-2 (25 entities, 261 permission flows, 252 permissions). While specific details cannot be disclosed due to data security protocols, both misconfigurations feature at least one transitive PE with paths of five or more steps, posing significant detection challenges under a limited query budget.